Globin-coupled sensors: A class of heme-containing sensors in Archaea and Bacteria

Shaobin Hou*, Tracey Freitas*, Randy W. Larsen†, Mikhail Piatibratov*, Victor Sivozhelezov*, Amy Yamamoto*, Ella A. Meleshkevitch‡, Mike Zimmer§, George W. Ordal§, and Maqsudul Alam*¶‖

Departments of *Microbiology and †Chemistry, University of Hawaii, Honolulu, HI 96822; ‡Whitney Laboratory, University of Florida, St. Augustine, FL 32080; §Department of Biochemistry, University of Illinois, Urbana, IL 61801; and ¶Marine Bioproducts Engineering Center, Honolulu, HI 96822

Edited by Harry B. Gray, California Institute of Technology, Pasadena, CA, and approved May 22, 2001 (received for review April 13, 2001)

The recently discovered prokaryotic signal transducer HemAT, which has been described in both *Archaea* and *Bacteria*, mediates aerotactic responses. The N-terminal regions of HemAT from the archaeon *Halobacterium salinarum* (HemAT-*Hs*) and from the Gram-positive bacterium *Bacillus subtilis* (HemAT-*Bs*) contain a myoglobin-like motif, display characteristic heme–protein absorption spectra, and bind oxygen reversibly. Recombinant HemAT-*Hs* and HemAT-*Bs* shorter than 195 and 176 residues, respectively, do not bind heme effectively. Sequence homology comparisons and three-dimensional modeling predict that His-123 is the proximal heme-binding residue in HemAT from both species. The work described here used site-specific mutagenesis and spectroscopy to confirm this prediction, thereby providing direct evidence for a functional domain of prokaryotic signal transducers that bind heme in a globin fold. We postulate that this domain is part of a globin-coupled sensor (GCS) motif that exists as a two-domain transducer having no similarity to the PER-ARNT-SIM (PAS)-domain superfamily transducers. Using the GCS motif, we have identified several two-domain sensors in a variety of prokaryotes. We have cloned, expressed, and purified two potential globin-coupled sensors and performed spectral analysis on them. Both bind heme and show myoglobin-like spectra. This observation suggests that the general function of GCS-type transducers is to bind diatomic oxygen and perhaps other gaseous ligands, and to transmit a conformational signal through a linked signaling domain.

proximal histidine | transducer

Globins are heme-containing proteins that are involved in binding and/or transport of diatomic oxygen. Presently, more than 700 globin sequences are known (1). It has been proposed that all globins have evolved from an ancestral redox protein of about 17 kDa that displayed the globin fold, which is characterized by the presence of eight helices, designated A through H (2). The residues absolutely conserved among all globins are the proximal histidine in the F helix (F8) and phenylalanine in the CD region (CD1) (3, 4). Highly conserved residues include the distal histidine in the E helix (E7), phenylalanine in the CD4 region, and proline at the beginning of the C helix (C2).

We recently discovered heme-containing transducers in the archaeon *Halobacterium salinarum* (HemAT-*Hs*) and the Gram-positive bacterium *Bacillus subtilis* (HemAT-*Bs*). These proteins bind diatomic oxygen and mediate an aerotactic response (5). The N termini of these transducers resemble myoglobin, and their C termini are homologous to the cytoplasmic signaling domain of bacterial chemoreceptors. We have also described three-dimensional homology models of the putative oxygen-sensing domain of HemATs (6). In these models the overall globin topology, including the orientation of the heme prosthetic group, is preserved, as is the hydrophobic core of the heme-binding pocket and the electrostatic stabilization of the CD region. Therefore, an experimental determination of the organization of the heme-binding pocket is of particular interest because this domain regulates the activity of the signaling domain in response to the binding of oxygen.

In this study we aimed to identify the regions of HemATs required for heme binding. To localize the minimal heme-binding region, we generated several C-terminal truncated derivatives of HemATs. The HemAT-Hs_{195} and HemAT-Bs_{176} fragments retained the heme- and oxygen-binding properties of the respective native proteins, whereas shorter versions of either protein did not bind heme effectively. We also determined the effect of replacing each histidine in these fragments with alanine and identified His-123 as the proximal heme-binding residue in both HemATs. Using this information, we constructed a 90-residue myoglobin-like domain transducer motif and identified several globin-coupled two-domain sensors in a variety of prokaryotes. We then cloned, expressed, purified, and performed spectral analysis of globin-coupled sensors (GCSs) from *Caulobacter crescentus* and *Thiobacillus ferrooxidans*. Both of them bind heme and show myoglobin-like spectra. We propose that globin-coupled sensors are a class of two-domain transducers having no similarity to the PER-ARNT-SIM (PAS)-domain superfamily transducers (7–10).

Materials and Methods

Strains. *Escherichia coli* competent cells JM109 from Promega were used for vector transformation. BL21(DE3) pLysS cells from Novagen were used for expression of the recombinant proteins. TOP10 cells from Invitrogen were used for TOPO PCR cloning.

Homology Modeling and Sequence Extraction and Alignment. Homology modeling of HemATs was performed according to Hou (6). Using the BLAST program (11), the entire nonredundant database at the National Center for Biotechnology Information (http://www.ncbi.nlm.nih.gov/blast) was searched. Sequencing of *C. crescentus, Bacillus anthracis* and *T. ferrooxidans* was accomplished at The Institute of Genomic Research (TIGR) (http://www.tigr.org). Sequencing of *Bordetella bronchiseptica* and *Bordetella pertussis* was performed at the Sanger Centre (http://www.sanger.ac.uk). Subsequent BLAST searches were performed on the finished and unfinished genomic sequences at TIGR and the Sanger Centre. Extracted sequences were initially aligned by using CLUSTALX (Windows-based version of CLUSTALW is available at ftp://ftp.ebi.ac.uk/pub/software/dos/clustalw/clustalx) and were manually adjusted by using MegAlign (DNAStar, Madison, WI).

MICROBIOLOGY

This paper was submitted directly (Track II) to the PNAS office.

Abbreviations: GCS, globin-coupled sensor; PAS, PER-ARNT-SIM; SWMb, sperm whale myoglobin; TIGR, The Institute of Genomic Research.

‖To whom reprint requests should be addressed. E-mail: alam@hawaii.edu.

The publication costs of this article were defrayed in part by page charge payment. This article must therefore be hereby marked "*advertisement*" in accordance with 18 U.S.C. §1734 solely to indicate this fact.

Construction of HemAT-*Hs* and HemAT-*Bs* Truncations. C-terminal six-His-tagged HemAT-*Hs* and HemAT-*Bs* truncations were constructed by a two-step PCR strategy. *Nde*I top primer and a site-specific primer were used in the first PCR to amplify different lengths of gene fragments. For HemAT-*Hs*, four different gene fragments encoding polypeptide fragments were created. Site-specific primer sequences are listed as follows: *hemAT-Hs*$_{185}$ (5′-GTGGTGGTGGTGGTGGTGTGCGATCT-GCTGATCGAAGGTCAACAGC-3′), *hemAT-Hs*$_{190}$ (5′-GTGGTGGTGGTGGTGGTGGATGTAGGTGTCCA-TTGCGATCTGC-3′), *hemAT-Hs*$_{195}$ (5′-GTGGTGGTGGTG-GTGGTGCTGGGCGTACGAGTCGATGTAGGTG-3′), and *hemAT-Hs*$_{200}$ (5′-GTGGTGGTGGTGGTGGTGCTCGTCGT-GGAGGCGCTGGGCGTACG-3′). For HemAT-*Bs*, three different polypeptide fragments were created. Site-specific primers are AS FOLLOWS: *hemAT-Bs*$_{171}$ (5′-TTAGTGGTGGTGGT-GGTGGTGTAAGTTCAAGATTTTTGTTGTTGC-3′), *he-mAT-Bs*$_{176}$ (5′-TTAGTGGTGGTGGTGGTGGTGGACAA-GCTGCTGTTCTAAGTTCAAG-3′), and *hemAT-Bs*$_{180}$ (5′-TTAGTGGTGGTGGTGGTGGTGTTAAAACGCTTA-AAGGACAAGC-3′). The PCR products were subcloned into *E. coli* expression vector pET3a.

Construction of N-Terminal His-Tagged HemAT-*Hs* and Its Histidine Mutation Derivatives. A recombinant gene fragment encoding the N-terminal His-tag HemAT-*Hs* construction (12) was used as the template for PCR site-directed mutagenesis. Individual histidine mutants were generated by using the QuickChange Site-Directed Mutagenesis protocol (Stratagene). Each mutated *hemAT-Hs* in pET14b vector was confirmed by DNA sequencing. Final constructions containing individual mutations were transformed into *E. coli* pLysS cells for expression.

Construction of C-Terminal His-Tagged HemAT-*Bs* and Its Histidine Mutation Derivatives. A recombinant *hemAT-Bs* gene was constructed by using a two-step PCR strategy. In the first PCR step, a six-His codon was fused to the *hemAT-Bs* in front of the stop codon. In the second PCR step, a *Bam*HI restriction site was introduced at the 3′ end of the gene. A TOPO cloning kit (Invitrogen) was used to clone the PCR product. *Nde*I/*Bam*HI restriction sites were used to subclone the *hemAT-Bs*$_{\text{C-6x-His}}$ fragment into the *E. coli* expression vector pET3a. This construction was used as a template for site-directed mutagenesis PCR according to the procedure described above. Mutated genes were confirmed by DNA sequencing and the final vectors were transformed into the *E. coli* pLysS cells for expression.

Cloning and Construction of Putative GCS Gene Expression Vectors. Genomic DNAs of *C. crescentus* and *T. ferrooxidans* were purchased from the American Type Culture Collection. Putative GCS genes were amplified by PCR. The primers are listed as follows. For *C. crescentus* 5′-GGCATATGGTCAACCAAT-TCTTACCAGCGAGTCGG-3′ and 5′-CTAGTGGTGGTG-GTGGTGGTGGCGCCCGGGACGGGCGAAAGCGGC-3′; for *T. ferrooxidans* 5′-CGCATATGATCTTGATCGATT-GAAAAAAGC-3′ and 5′-TAGTGGTGGTGGTGGTGGT-GCTTGGCCGGCAAGTCGTCGCAG-3′. The final PCR products were cloned into a TOPO vector, and genes were subcloned into *E. coli* expression vector pET3a.

Expression and Purification of Recombinant HemATs and Putative GCSs in *E. coli*. Expression and one-step purification of HemATs, their histidine mutant derivatives, truncated HemATs, and putative GCSs were performed according to Piatibratov *et al.* (12).

Overexpression of HemAT-H123A in Their Native Hosts. *hemAT-Hs*/pKJ427 and *hemAT-Bs*/pEB112 constructions (5) were used as templates for PCR site-directed mutagenesis of His-123 as described above. Mutations were confirmed by DNA sequencing, and vectors carrying mutated genes were then transformed into the *H. salinarum* Δ*hemAT-Hs* strain and *B. subtilis* Δ*ten* strain (5) by using standard halobacterial and *B. subtilis* transformation procedures (5).

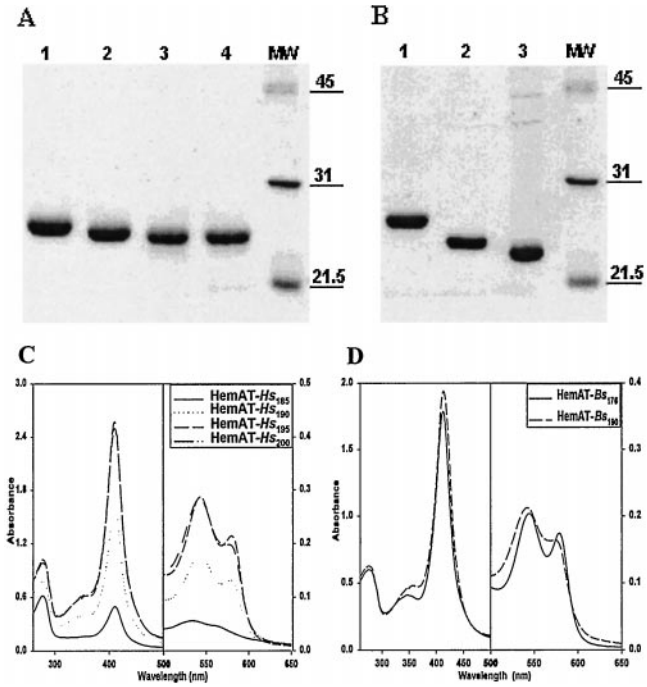

Fig. 1. Heme-binding properties of purified fragments of recombinant HemAT-*Hs* and HemAT-*Bs*. (*A* and *B*) Recombinant fragments in SDS/PAGE. (*A*) Lanes: 1, HemAT-*Hs*$_{200}$; 2, HemAT-*Hs*$_{195}$; 3, HemAT-*Hs*$_{190}$; 4, HemAT-*Hs*$_{185}$. (*B*) Lanes: 1, HemAT-*Bs*$_{180}$; 2, HemAT-*Bs*$_{176}$; 3, HemAT-*Bs*$_{171}$. MW, molecular weight standards ($\times 10^{-3}$). (*C* and *D*) Absorption spectra of recombinant fragments. (*C*) HemAT-*Hs*$_{200}$, HemAT-*Hs*$_{195}$, HemAT-*Hs*$_{190}$, HemAT-*Hs*$_{185}$; the protein concentration was 0.50 mg/ml. (*D*) HemAT-*Bs*$_{180}$, HemAT-*Bs*$_{176}$; protein concentration was 0.42 mg/ml. Spectra were measured in 200 mM NaCl/50 mM Na_2HPO_4 (pH 8.0).

SDS/PAGE and Heme Staining. The purified HemAT and truncation samples were analyzed by modified dimethoxy-benzidine heme staining as described by Piatibratov *et al.* (12).

Determination of Protein Concentration and Heme Content. Protein concentrations were determined by using the Pierce Coomassie Plus Protein Assay Reagent kit according to the manufacturer's protocol. The heme content of purified HemATs was determined by the alkaline hematin method (13).

Results

Identification of the Oxygen-Binding Domains of HemAT-*Hs* and HemAT-*Bs*. We began by generating fragments of *hemAT-Hs* that encode polypeptides spanning the first 185, 190, 195, and 200 residues, respectively, of the normal gene product. These recombinant proteins were constructed with N-terminal His tags and were purified (Fig. 1*A*). The effect of C-terminal truncation was explored by examining their absorption spectra in the near-UV and visible region for peaks characteristic of oxygen-bound heme proteins. Fragments HemAT-*Hs*$_{195}$ and HemAT-*Hs*$_{200}$ bound heme more effectively than the shorter fragments. In particular, HemAT-*Hs*$_{185}$ displayed relatively little heme binding as indicated by the low absorption peak at 410 nm (Fig. 1*C*). The low absorption peak of this polypeptide may be due to

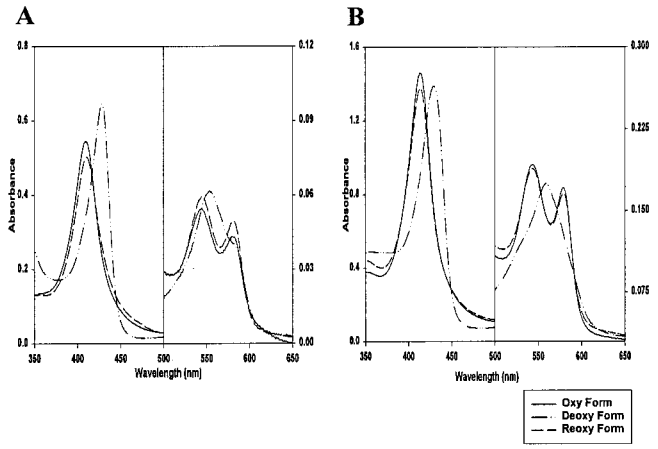

Fig. 2. HemAT-Hs_{195} and HemAT-Bs_{176} bind oxygen reversibly. (*A*) HemAT-Hs_{195}. (*B*) HemAT-Bs_{176}. Spectra were measured in 200 mM NaCl/50 mM Na_2HPO_4 (pH 8.0).

changes in the conformation of the heme-binding pocket or to improper folding of the domain.

Similarly, we generated His-tagged fragments of *hemAT-Bs* that encode polypeptides spanning the first 171, 176, and 180 residues of the protein (Fig. 1*B*). HemAT-Bs_{171} formed inclusion bodies and required 6–8 M urea to solubilize. Therefore, absorption spectra were determined only with the other two fragments (Fig. 1*D*). As seen previously with full-length HemAT-*Bs*, the oxygen-bound forms of these fragments were relatively short lived, converting to the met [Fe(III)] form after about 5 h at room temperature and after about 24 h at 4°C. The spectra of the met forms were very similar to that of the met form of hemoglobin from *Paramecium* (14) and cyanobacteria (15). In contrast, the oxygen-bound form of HemAT-Hs_{195} has a lifetime of 24–48 h at room temperature and of several weeks at 4°C (data not shown).

HemAT-Hs_{195} and HemAT-Bs_{176} Bind Oxygen Reversibly. Both HemAT-Hs_{195} and HemAT-Bs_{176} have absorption spectra typical of oxygen-bound heme proteins, with maxima at 410 nm (Soret), 580 nm (α band), and 542 nm (β band) (Fig. 2 *A* and *B*). After deoxygenation with sodium dithionite, the Soret bands of both fragments shifted to 428 nm, and the α and β bands converged to a broad peak at 554 nm for HemAT-Hs_{195} and 560 nm for HemAT-Bs_{176}. This behavior is consistent with the formation of the deoxygenated forms and is similar to the effect seen with deoxymyoglobin (5). When the deoxygenated forms of HemAT-Hs_{195} and HemAT-Bs_{176} were reexposed to atmospheric oxygen, their absorption spectra reverted to that of the oxygenated forms (Fig. 2 *A* and *B*). Thus, both HemAT-Hs_{195} and HemAT-Bs_{176} behave like other well characterized, heme-containing proteins and exhibit a reversible oxygen-binding capacity such as that seen with their full-length counterparts (5). We measured the oxygen-binding affinities of HemAT-*Hs* and HemAT-*Bs*. The association constants for oxygen binding to both HemAT-*Hs* and HemAT-*Bs* are 8×10^6 M^{-1} and 4×10^5 M^{-1}, respectively, as compared with 1.2×10^6 M^{-1} for sperm whale myoglobin (SWMb) and 2.0×10^4 M^{-1} for RmFixLH (16).

His-123 Is the Proximal Residue in Both HemATs. All globins have a histidine residue that binds directly to the fifth coordinate of the heme iron. The His-123 residue in both HemAT-*Hs* and HemAT-*Bs* can be aligned with this histidine residue (His-93, F8) in myoglobin (5). We generated models of the three-dimensional structures of HemAT-Hs_{195} and HemAT-Bs_{176} (Fig. 3 *A* and *C*)

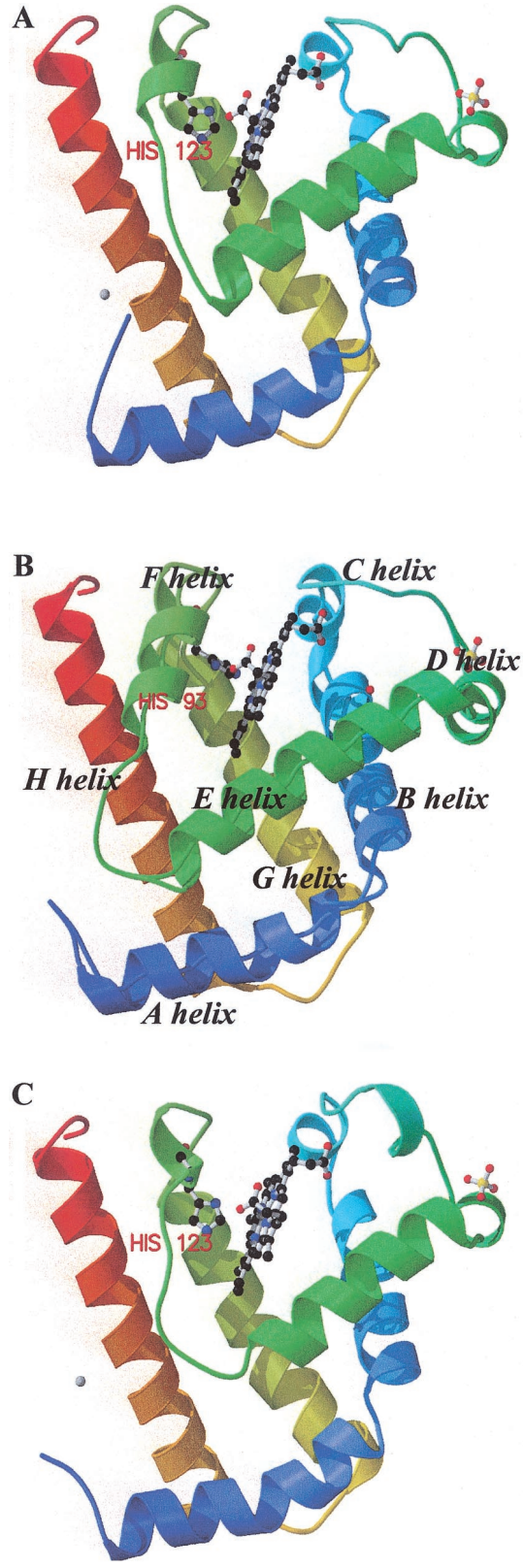

Fig. 3. Homology models of the heme-binding domains of HemAT-*Hs* and HemAT-*Bs* compared with the known structure of SWMb. The putative heme-binding domains of HemAT-Hs_{195} (*A*) and HemAT-Bs_{176} (*C*), and the crystal structure of the heme-binding domain of SWMb (*B*) are shown. The side chain of the histidine residue (His-123 in HemAT-*Hs* and HemAT-*Bs*, His-93 in SWMb) that coordinates with the heme iron is shown for each molecule.

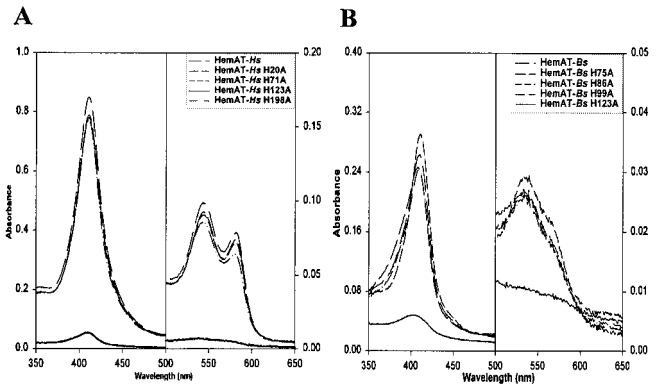

Fig. 4. Absorption spectra of purified recombinant HemAT fragments and their histidine-to-alanine derivatives. (*A*) HemAT-*Hs* and its mutant derivatives. (*B*) HemAT-*Bs* and its mutant derivatives. Spectra were measured in 200 mM NaCl/50 mM Na_2HPO_4 (pH 8.0).

based on the overall fold of myoglobin (Fig. 3*B*). The side chain of the relevant heme-binding histidine residue is shown in each structure along with the heme prosthetic group itself. The models for HemAT-Hs_{195} and HemAT-Bs_{176} are both consistent with the idea that His-123 is the residue that directly contacts the heme iron.

To determine experimentally whether His-123 is involved in heme binding, the four histidine residues in the N-terminal domains of HemAT-*Hs* (His-20, His-71, His-123, and His-198) and HemAT-*Bs* (His-75, His-86, His-99, and His-123) were changed to alanine residues by site-directed mutagenesis. Modified heme-specific staining was performed on these proteins after subjecting them to nondenaturing PAGE. Heme staining was observed with the wild-type protein and all of the mutant proteins from both species except for the Ala-123 variants (data not shown).

Fig. 4 shows the optical properties of purified HemAT-*Hs* and HemAT-*Bs* and their alanine-substituted derivatives. The spectra for most of the variants resemble those of the parental proteins, but both of the Ala-123 mutant proteins lack the characteristic spectral features associated with heme binding. The Ala-123 proteins did have a low absorbance near 410 nm that might be attributable to nonspecific heme binding. In capillary assays, no aerotactic response was observed with either *H. salinarum* or *B. subtilis* strains expressing the respective Ala-123 proteins, whereas the other mutant proteins exhibited aerotactic responses similar to those of cells producing the corresponding wild-type proteins (data not shown). Taken together, these data provide compelling support for the identity of His-123 as the proximal heme-binding residue in both HemATs.

GCS Motif. The heme-containing oxygen sensors FixL (17, 18) and Dos (19) are members of the PAS-domain superfamily (7–10). The PAS domain has a distinctive fold with a six-stranded β sheet, and different proteins containing this domain are known to sense redox potential, oxygen, proton motive force, or light. However, HemAT proteins do not contain a PAS domain. We speculated that the oxygen-sensing globin-fold domain of HemAT could be more widespread than previously thought. To test this idea, we designed a 90-residue template that contains the globin-coupled transducer motif. This sequence was used to search for potential two-domain GCSs. A critical feature of the GCS motif is the spacing between the highly conserved phenylalanine in the CD1 region and the highly conserved histidine at the F8 position (3).

We performed a BLAST search with this GCS motif in all available genome databases and found six additional HemAT homologs (Fig. 5*A*). The *C. crescentus*, *B. anthracis*, and *Bacillus halodurans* homologs are classified as methyl-accepting chemotaxis proteins, and an alignment of the highly conserved signaling domain diagnostic for these proteins is shown in Fig. 5*B*. The remaining proteins showing the GCS motif include putative histidine kinase from *Bordetella* spp. and phosphodiesterase from *T. ferrooxidans*. Members of this last group of proteins contain potential diguanylate cyclase/phosphodiesterase domains (Fig. 5*C*). We cloned, expressed, purified, and performed spectral analysis of two predicted GCSs from *C. crescentus* and *T. ferrooxidans*. Both displayed similar absorption spectra in the near-UV and visible regions, as is characteristic of oxygen-bound heme proteins (Fig. 5*D*).

Discussion

Myoglobin folds into a single monomeric, globular domain that contains eight α-helices and one high-affinity heme-binding site. The work presented here identified a similar heme-binding unit in archaeal and bacterial aerotaxis transducers, which we call HemATs. The N-terminal 195 residues of HemAT from the archaeon *H. salinarum* (HemAT-Hs_{195}) and the 176 N-terminal residues of HemAT from the Gram-positive bacterium *B. subtilis* (HemAT-Bs_{176}) comprise minimal domains that bind heme as effectively as the full-length proteins. These sequences coincide approximately with the regions in which the HemATs can be aligned with the myoglobin sequence (5).

The function of His-123 as the primary heme-binding residue in both HemAT-*Hs* and HemAT-*Bs* distinguishes these proteins from the CooA CO sensors, which contain a thiolate ligand in the Fe(III) state and a histidine-bound ligand in the Fe(II) state (20, 21). Other heme-based sensors, such as FixL and guanylate cyclase, bind heme exclusively through coordination with histidine (20). The structural homology between HemAT and SWMb is apparent when the amino acid sequences are aligned (5). His-123 of HemATs is in a position corresponding to the heme-binding His (F8) of SWMb. Using this alignment, helical regions in HemATs can be assigned and shown to correspond to the A, B, C, D, E, F, G, and H helices of SWMb. HemATs also contain loop regions connecting the helical domains, although their length varies significantly from the length of the loops in SWMb (6). Identification of this structural homology depends critically on the demonstration that His-123 is the proximal heme-binding residue in HemAT.

None of the previously described heme-based sensors, including FixL (O_2 sensor), soluble guanylate cyclase (NO sensor), Dos protein (O_2 sensor), and CooA protein (CO sensor) use the globin fold (18, 19, 20). HemAT-*Hs* and HemAT-*Bs* are thus, to our knowledge, the first group of heme-based sensors shown to employ the globin motif and to couple it to the signaling functions of the methyl-accepting chemotaxis proteins. The GCS motif that we describe also identified two additional proteins that are thought to be a histidine kinase and a phosphodiesterase, respectively. The spectral properties of GCS from *C. crescentus* and *T. ferrooxidans* indeed confirmed our prediction of the existence of a GCS class. Thus, the presence of HemAT homologs in divergent microorganisms (from Archaea to Bacteria) indicates that GCSs are likely to be early arising components during evolution of the sensory arsenal of life.

Our data are consistent with a two-domain model for globin-coupled sensors. In the case of HemATs, the N-terminal domain serves as an oxygen sensor by virtue of its bound heme, whereas the C-terminal domain shows homology to chemotactic signal transducers (Fig. 5*B*) and presumably interfaces with the pathway that controls motility. This transducer-like domain begins at residue 222 for HemAT-*Hs* and at residue 198 for HemAT-*Bs*. We postulate that the intervening "linker regions" are involved

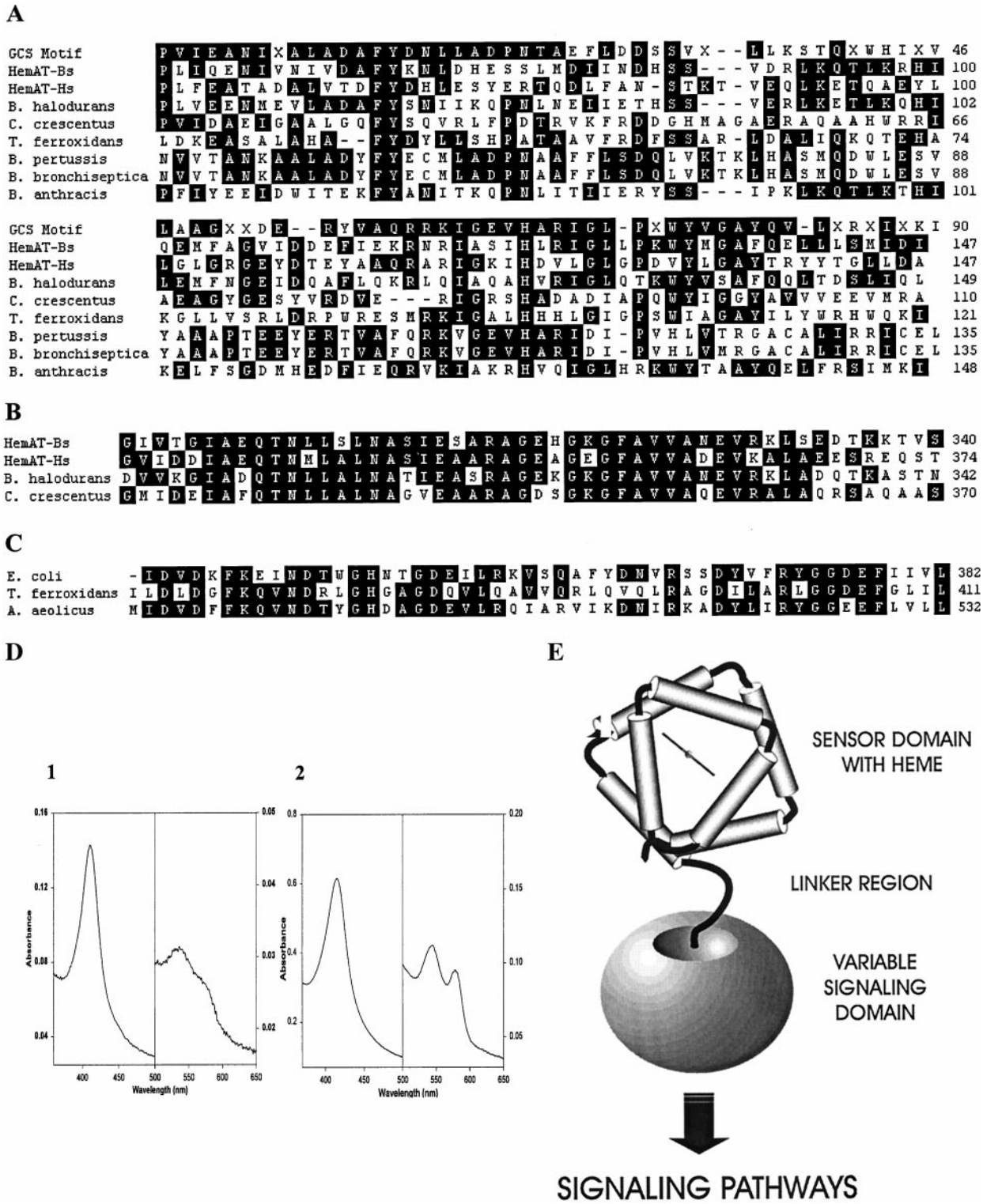

Fig. 5. Identification of GCSs. (*A*) Alignment of the GCS motif with the heme-binding globin-fold regions of TIGR 1392 (*B. anthracis*), HemAT-*Bs*, HemAT-*Hs*, BAB04224.1 (*B. halodurans*), TIGR 12574 (*C. crescentus*), Sanger 518 (*B. bronchiseptica*), Sanger 520 (*B. pertussis*), and TIGR 6137 (*T. ferrooxidans*). Black boxes highlight residues identical to the GCS consensus. (*B*) Alignment of the highly conserved signaling domain in the C-terminal regions of HemAT-*Bs*, HemAT-*Hs*, BAB04224.1 (*B. halodurans*), and TIGR 12574 (*C. crescentus*). (*C*) Alignment of a homologous sequence in the C-terminal regions of AE005356 (*E. coli*) and TIGR 6137 (*T. ferrooxidans*) with the putative diguanylate cyclase/phosphodiesterase GGDEF domain of Aq 563 (*Aquifex aeolicus*). (*D*) Absorption spectra of purified recombinant GCS from (*1*) *C. crescentus* and (*2*) *T. ferrooxidans.* (*E*) A unified working model of the GCS.

in communication between the sensing and signaling domains, probably through propagation of conformational changes initiated upon binding oxygen to heme (Fig. 5*E*).

In summary, we propose that the GCS represents a class of sensors distinct from the PAS-domain superfamily. These sensors may have evolved as two-domain proteins with the

capacity to sense diatomic oxygen and other gaseous ligands through a sensor domain that binds heme with globin fold. The sensor domain transmits the information of ligand binding to the rest of the cell through a variety of linked signaling domains (Fig. 5E).

We thank Gerald Hazelbauer, Mike Manson, Sandy Parkinson, Barry Taylor, Paul Patek, and JoAnn Radway for helpful comments on the manuscript. We also thank Hyung Suk Yu, Claude Belisle, and Summer Lum for participation in different stages of protein purification. This investigation was supported by National Science Foundation Grant MSB-087124 and by a University of Hawaii intramural grant to M.A.

1. Kapp, O. H., Moens, L., Vanfleteren, J., Trotman, C. N., Suzuki, T. & Vinogradov, S. N. (1995) *Protein Sci.* **4,** 2179–2190.
2. Moens, L., Vanfleteren, J., Van de Peer, Y., Peters, K., Kapp, O., Czeluzniak, J., Goodman, M., Blaxter, M. & Vinogradov, S. N. (1996) *Mol. Biol. Evol.* **13,** 324–333.
3. Bashford, D., Chothia, C. & Lesk, A. M. (1987) *J. Mol. Biol.* **196,** 199–216.
4. Vinogradov, S. N., Walz, D. A. & Pohajdak, B. (1992) *Comp. Biochem. Physiol.* **103,** 759–773.
5. Hou, S., Larsen, R. W., Boudko, D., Riley, C. W., Karatan, E., Zimmer, M., Ordal, G. W. & Alam, M. (2000) *Nature (London)* **403,** 540–544.
6. Hou, S. (2000) Ph.D. thesis (Univ. of Hawaii, Honolulu).
7. Taylor, B. L. & Zhulin, I. B. (1999) *Microbiol. Mol. Biol. Rev.* **63,** 479–506.
8. Zhulin, I. B. & Taylor, B. L. (1998) *Mol. Microbiol.* **29,** 1522–1523.
9. Zhulin, I. B., Taylor, B. L. & Dixon, R. (1997) *Trends Biochem. Sci.* **22,** 331–333.
10. Gong, W., Hao, B., Mansy, S. S., Gonzalez, G., Gilles-Gonzalez, M. A. & Chan, M. K. (1998) *Proc. Natl. Acad. Sci. USA* **95,** 15177–15182.
11. Altschul, S. F., Gish, W., Miller, W., Myers, E. W. & Lipman, D. J. (1990) *J. Mol. Biol.* **215,** 403–410.
12. Piatibratov, M., Hou, S., Brooun, A., Yang, J., Chen, H. & Alam, M. (2000) *Biochim. Biophys. Acta* **1524,** 149–154.
13. Zander, L., Lang, W. & Wolf, H. (1984) *Clin. Chim. Acta* **136,** 83–93.
14. Tsubamoto, Y., Matsuoka, A., Yusa, K. & Shikama, K. (1990) *Eur. J. Biochem.* **193,** 55–59.
15. Thorsteinsson, M. V., Bevan, D. R., Ebel, R. E., Weber, R. E. & Potts, M. (1996) *Biochim. Biophys. Acta* **1292,** 133–139.
16. Gilles-Gonzalez, M. A., Gonzalez, G. & Perutz, M. F. (1994) *Biochemistry* **33,** 8067–8073.
17. Gilles-Gonzalez, M. A., Ditta, G. S. & Helinski, D. R. (1991) *Nature (London)* **350,** 170–172.
18. Monson, E. K., Weinstein, M., Ditta, G. S. & Helinski, D. R. (1992) *Proc. Natl Acad. Sci. USA* **89,** 4280–4284.
19. Delgado-Nixon, V. M., Gonzalez, G. & Gilles-Gonzalez, M. A. (2000) *Biochemistry* **39,** 2685–2691.
20. Rodgers, K. R. (1999) *Curr. Opin. Chem. Biol.* **3,** 158–167.
21. Shelver, D., Kerby, R. L., He, Y. & Roberts, G. P. (1997) *Proc. Natl. Acad. Sci. USA* **94,** 11216–11220.